Sand Behavior Induced by High-Speed Penetration of Projectile

Keiko Watanabe[*], Koichi Tanaka[**], Keisuke Iwane[*], Syungo Fukuma[*],
Kazuyoshi Takayama[***] and Hidetoshi Kobayashi[*]

[*] Department of Mechanical Science and Bioengineering, Osaka University,
1-3 Machikaneyama, Toyonaka, Osaka, 560-8531, Japan.
e-mail: keikow@me.es.osaka-u.ac.jp
[**] Department of Mechanical Engineering, Chubu University,
[***] Institute of Fluid Science, Tohoku University

Abstract: The primary objective is establishing tangible experimental methods and data analyzing methods in order to grasp various phenomena, which were the behavior of ejecta and projectile, the penetration depth and speed of projectile, fractured grains and the pressure distribution, induced by high-speed impact of projectile on sand. The plate impact experiments were conducted using vertical powder gun. The principal results are summarized as follows: Sands around the penetrated projectile were smashed to fine powder of 5 μm or less like a potato starch. Circumferential crashed sands were conically distributed and generated at impact velocity above 300 m/s. Conical massive crashed sand was produced ahead of projectile and vertical angle converged to around 60° as the velocity increases. The projectile penetrated at a speed about equal to the impact velocity in the initial penetration and decelerated rapidly over since.

1. INTRODUCTON

Collisions between geological materials and rigid bodies occur in various situations, which are excavation, construction, military application and asteroid impact. Accordingly, the impact and penetration of projectiles in soil have long been studied extensively[1-8]. However, for geological particulate materials such as sand, because the particle behavior is so complicated due to heterogeneity and instability of granular media, there have been few experiments investigating the impulse loading of these media, and the penetration properties on them are less understood. Dynamics of projectile penetration into sand depends greatly on the features of motion and state of the sand material at the interface with the projectile.

The final goal of this study is to develop an understanding of behavior of projectile during penetration, condition and distribution of comminuted sands and pressure distribution in sand under the impulse loading. As the first step, the primary objective is establishing tangible experimental methods and data analyzing methods in order to grasp various phenomena induced by high-speed impact of projectile on sand.

Report Documentation Page	*Form Approved* *OMB No. 0704-0188*

Public reporting burden for the collection of information is estimated to average 1 hour per response, including the time for reviewing instructions, searching existing data sources, gathering and maintaining the data needed, and completing and reviewing the collection of information. Send comments regarding this burden estimate or any other aspect of this collection of information, including suggestions for reducing this burden, to Washington Headquarters Services, Directorate for Information Operations and Reports, 1215 Jefferson Davis Highway, Suite 1204, Arlington VA 22202-4302. Respondents should be aware that notwithstanding any other provision of law, no person shall be subject to a penalty for failing to comply with a collection of information if it does not display a currently valid OMB control number.

1. REPORT DATE **07 FEB 2011**	2. REPORT TYPE **Final**	3. DATES COVERED **19-03-2009 to 18-03-2010**
4. TITLE AND SUBTITLE **Phenomenological studies of the response of granular and geological media to high-speed (Mach 1-5) projectiles**		5a. CONTRACT NUMBER **FA23860914011**
		5b. GRANT NUMBER
		5c. PROGRAM ELEMENT NUMBER
6. AUTHOR(S) **Tanaka Koichi**		5d. PROJECT NUMBER
		5e. TASK NUMBER
		5f. WORK UNIT NUMBER
7. PERFORMING ORGANIZATION NAME(S) AND ADDRESS(ES) **Chubu University,1200 Matsumoto-cho,Kasugai City 487-8501,Japan,NA,NA**		8. PERFORMING ORGANIZATION REPORT NUMBER **N/A**
9. SPONSORING/MONITORING AGENCY NAME(S) AND ADDRESS(ES) **AOARD, UNIT 45002, APO, AP, 96338-5002**		10. SPONSOR/MONITOR'S ACRONYM(S) **AOARD**
		11. SPONSOR/MONITOR'S REPORT NUMBER(S) **AOARD-094011**

12. DISTRIBUTION/AVAILABILITY STATEMENT   **Approved for public release; distribution unlimited**

13. SUPPLEMENTARY NOTES

14. ABSTRACT   **This is the final report of a project to grasp various phenomena induced by the high-speed impact of projectiles on sand. These were the behavior of ejecta and the projectile, the penetration depth and speed of the projectile, and fractured grains and pressure distribution.**

15. SUBJECT TERMS   **Solid Mechanics, penetration mechanics**

16. SECURITY CLASSIFICATION OF:			17. LIMITATION OF ABSTRACT	18. NUMBER OF PAGES	19a. NAME OF RESPONSIBLE PERSON
a. REPORT **unclassified**	b. ABSTRACT **unclassified**	c. THIS PAGE **unclassified**	**Same as Report (SAR)**	**8**	

Standard Form 298 (Rev. 8-98)
Prescribed by ANSI Std Z39-18

2. EXPERIMENT

Plate impact experiments were performed using vertical powder gun as shown in Fig.1. The projectiles with a mass of 12 or 12.5 g consisted of a plate impactor of stainless steel or brass 5 mm thick, 15 mm diameter, mounted on the front of a polycarbonate sabot as shown in Fig.2. The impact velocities investigated ranged from 150 to 1400 m/s.

The target was made up of quartz sands with a grain diameter of between 0.1 and 1 mm and a density of 2.65×10^3 kg/m^3. Grain size distribution was shown in Fig.3, and the grain size using in this experiment was 300~500 μm. The quartz sands were placed in three kinds of containers (see Fig.4 and Table 1). In the case of container B and C, the packing density was $1.49 \sim 1.56 \times 10^3$ kg/m^3, implying a porosity of 40~43 %.

Behavior of the ejecta and the projectile during initial penetration was visualized with high space and time resolutions using high-speed camera (MEMRECAM GX-8, NAC Image Technology Inc.) with 1,000 or 20,000 fps and ultra high-speed camera (ULTRA Cam HS-106E, NAC Image Technology Inc.) with 200,000 fps.
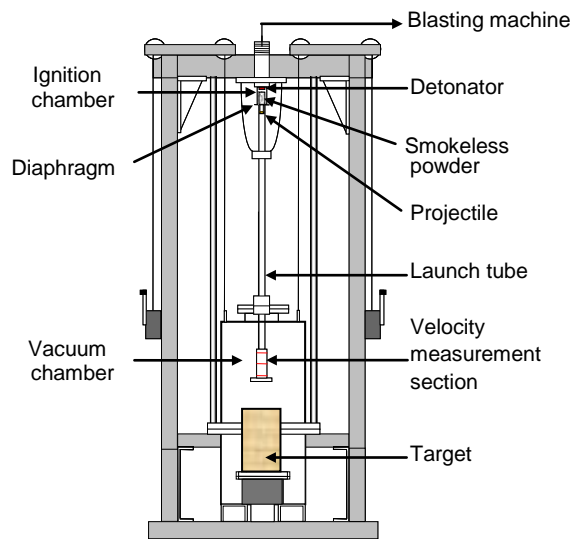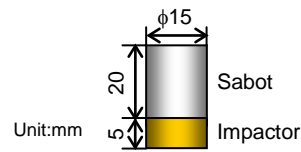

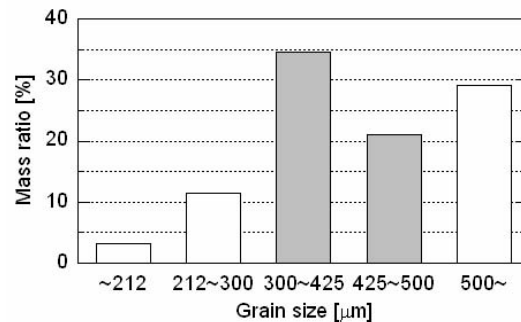Fig.1 Vertical powder gun.

Fig.2 Projectile.
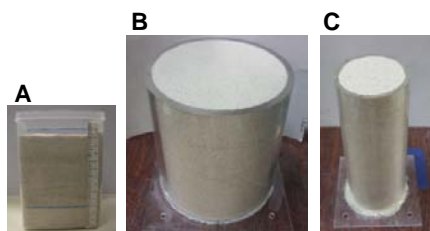

Fig.3 Grain size distribution.

Fig.4 Container.

Table 1 Material and size of containers.

Container	A	B	C
Material	Polyethylene	PMMA	PMMA
Inner dia. [mm]	(115x155x155)	φ80	φ190
Thickness [mm]	1	5	10
Height [mm]	125	200	200

The two-dimensional pressure distribution of the depth direction was measured using the pressure sensitive films (Prescale, Fujifilm Co.) that were placed between the sand aggregate and the inner surface of an acrylic cylindrical container. When pressure is applied, the microcapsules are broken and the color-forming material reacts with the color-developing material. Red patches appear on the film and the color density changes according to the various pressure levels.

Optical glass fibers were used to detect optically the arrival time and trajectory of projectile in sand. The schematic illustration is shown in Fig. 5. The thin silica/silica fiber (core diameter; 200 μm, clad diameter; 220 μm) was selected and polyimide jacket was removed by sulfuric acid so that the penetration of projectile is prevented from disturbing. LED (L6112-01, Hamamatsu Photonics K.K.) and Si PIN photodiode (S5971, Hamamatsu Photonics K.K.) were used as light source and photo sensor, respectively. Beams of LED were passed through optical glass fibers which were arranged at 20 mm intervals, and photo sensors detect them. When the beam is blocked by cutting of fiber due to penetration of the projectile, the arrival time of projectile is detected.
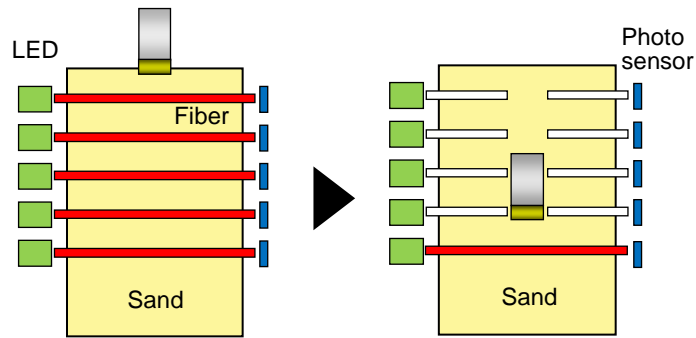

Fig.5 Schematic illustration of optical glass fiber detector.

3. RESULTS AND DISCUSSION

The investigation items to establish tangible experimental methods and data analyzing methods and results are summarized as follows:

3.1 High-Speed Visualization of Behavior of Ejecta and Projectile

Figure 6 shows continuous pictures of behavior of the ejecta from the surface of sand when the projectile penetrated into sand aggregate packed in container C at a speed of 350 m/s. Frame rate was 1,000 fps and exposure time was 50 μs. Sands were ejected radially like a crown and the velocity was about 20 m/s. It was found that the container wall greatly influenced the latter behavior of ejecta. Figure 7 shows continuous pictures of behavior of the projectile during initial penetration into sand aggregate packed in container C at a speed of 495 m/s. Frame rate was 20,000 fps and exposure time was 1 μs. Figure 8 shows detailed continuous pictures. Frame rate was 200,000 fps and exposure time was 300 ns. It was found that sands were at rest and the projectile penetrated at a speed about equal to the impact velocity in the initial penetration.
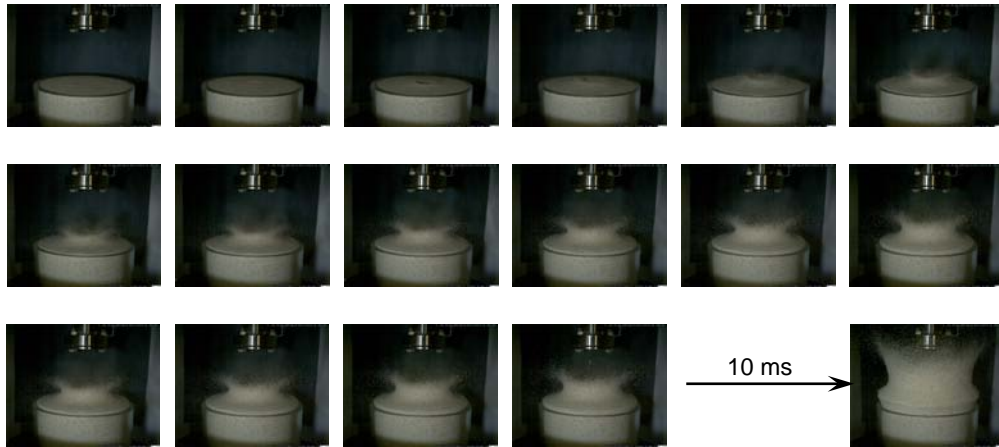
Fig.6 High-speed visualization of behavior of ejecta.
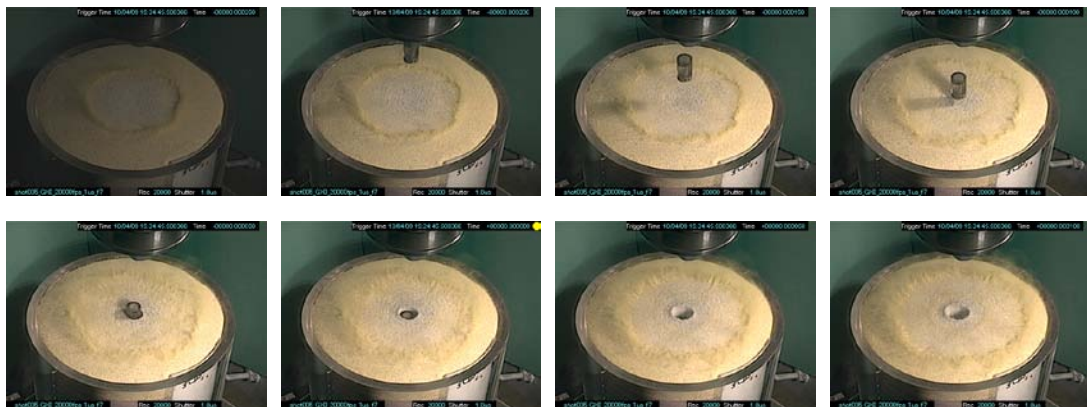Frame rate; 1,000 fps, exposure time; 50 μs, impact velocity; 350 m/s, container; C.

Fig.7 High-speed visualization of behavior of projectile during penetration.
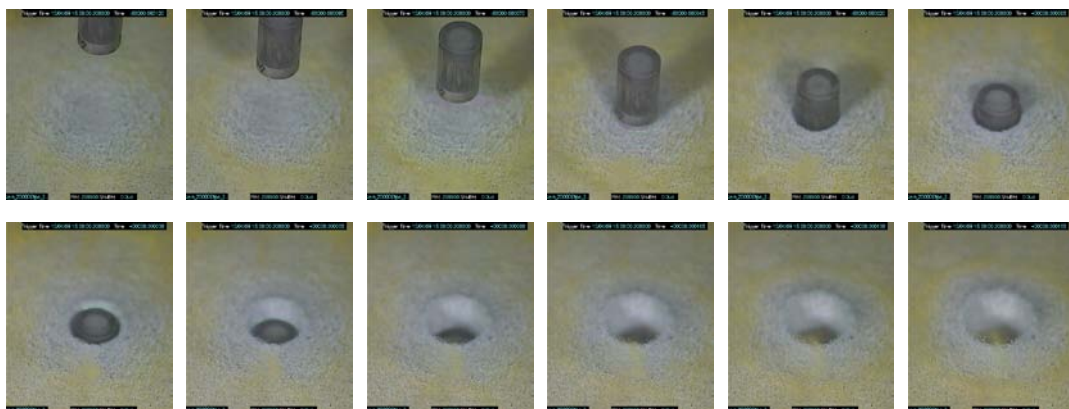Frame rate; 20,000 fps, exposure time; 1 μs, impact velocity; 495 m/s, container; C.

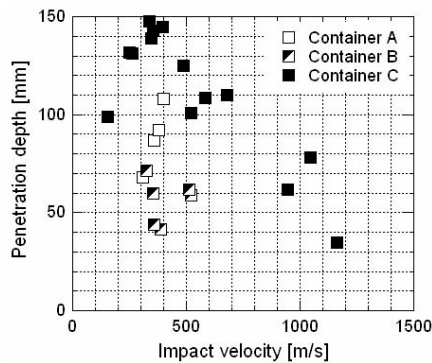Fig.8 High-speed visualization of detailed behavior of projectile during penetration.
Frame rate; 200,000 fps (every 5 frames), exposure time; 300 ns,
impact velocity; 495 m/s, container; C.

Fig.9 Effect of container type on relationship between impact velocity and penetration depth (impactor material; brass).
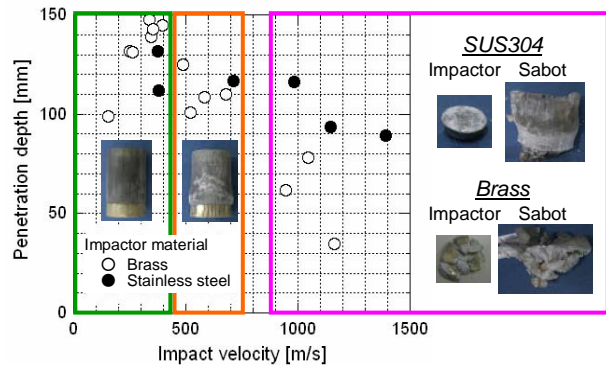
Fig.10 Effect of impactor material and deformation of projectile on relationship between impact velocity and penetration depth (container C).

3.2 Relationship between Impact Velocity and Penetration Depth

Figure 9 shows the effect of container type on the relationship between impact velocity and penetration depth. It was found that the relationship depended largely on the container types. In the case of container B, since the sand motion was strongly constrained by the container wall, the projectile didn't penetrate deeply and the container was broken to pieces over 600 m/s. Since container A made of polyethylene was easily deformed by applying a force, it was not fit to use. Figure 10 shows the effect of impactor material and deformation of projectile on the relationship between impact velocity and penetration depth. It was found that the degree of deformation of sabot and impactor greatly influenced the penetration depth. At a velocity below 450 m/s, the projectile did not change shape and the penetration depth increased with increasing the impact velocity. However, after 450 m/s, the projectile gradually began to deform and the penetration depth decreased with increasing the impact velocity. Especially, deformation of the brass impactor became large and the penetration depth was shallow in comparison with the stainless steel projectile.

## 3.3 Observation of Fractured Grains and Their Distribution

Sands around the penetrated projectile were smashed to fine powder of 5 μm or less like a potato starch as shown in Fig.11. It was found that there were two different kinds of distributions of crashed sands, which were circumferential and massive ahead of the projectile as shown in Fig.12. Circumferential crashed sands were powdery and generated at impact velocity above 300 m/s (see Fig.13). The distribution shape of circumferential crashed sands was an oblate cone (see the area inside thick line in Fig.14). On the other hand, the conical massive crashed sand was produced throughout all examined impact velocity range. Figure 15 shows the relationship between the vertical angle, 2α, of conical lump and the impact velocity. At a velocity below around 400 m/s, the vertical angle, 2α, decreased with increasing the impact velocity. However,

after around 400 m/s, the vertical angle, 2α, reached a constant when it reached about 60° and it did not increase any more even if the impact velocity increased. Figure 16 the relationship between the density of conical lump and the impact velocity. Upper line and lower line indicate the density of quartz (2.65×10^3 kg/m³) and the original packing density ($1.49 \sim 1.56 \times 10^3$ kg/m³), respectively. The density of conical lamp was approximately 2.0 to 2.6×10^3 kg/m³ regardless of variations in the impact velocity, and it was found that the conical massive crashed sand was firmly pressed and compressed.
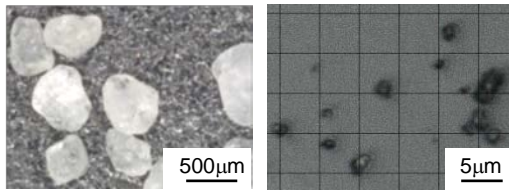
(a) Original sand   (b) Crashed sand

Fig.11 Microscopic photographs of sand.
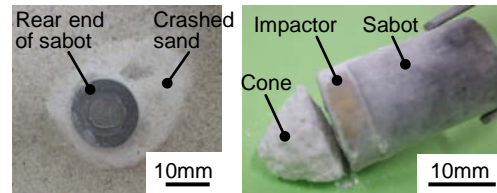
(a) Circumferential (b) Massive (ahead of projectile)

Fig.12 Distribution of crashed sand.

251680768252263424

(a) 250 m/s   (b) 521 m/s.

Fig.13 Effect of impact velocity on generation of circumferential crashed sand.
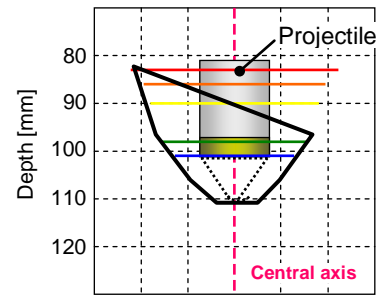

Fig.14 Measured cross-sectional distribution of crashed sand. Impact velocity; 521 m/s, penetration depth; 101 mm.
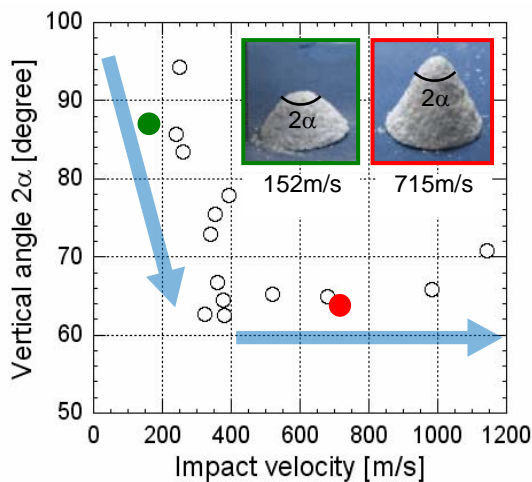

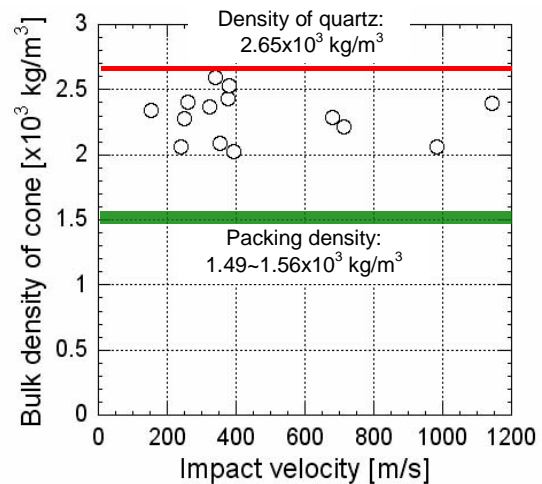Fig.15 Effect of impact velocity on shape of massive crashed sand.

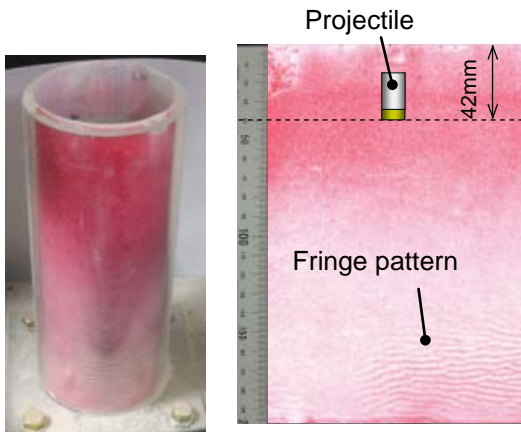Fig.16 Effect of impact velocity on density of massive crashed sand.

Fig.17 Two-dimensional pressure distribution
on the inner wall of container B.
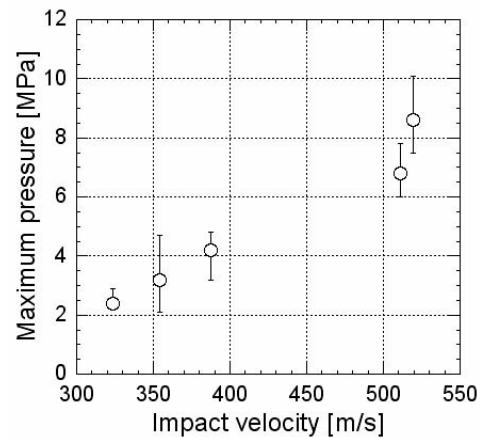Impact velocity; 389 m/s,
penetration depth; 42 mm.

Fig.18 Relationship between maximum
pressure and impact velocity
(container B).

3.4 Measurement of Two-Dimensional Pressure Distribution

Figure 17 shows the actual pressure sensitive film in container B at a speed of 389 m/s. The penetration depth was 42 mm. The region between from the rear end of the stopped projectile to 30mm away from the stop position of projectile became darker color. At the lower part, a fringe pattern was produced due to interference of stress waves reflected from the container wall. Figure 18 shows the relationship between the maximum pressure and impact velocity. The Maximum pressure increased with increasing the impact velocity. It is theoretically predicted that container B is broken when the inner pressure exceeds about 10 MPa, and it was actually broken apart over 600 m/s as was stated previously in section 3.2. This indicates that this pressure measurement method is applicable to the quantitative analysis.

3.5 Detection of Behavior of Projectile during Penetration

Figure 19 shows the result obtained by optical glass fiber detector in container C at a speed of 250 m/s. The penetration depth was 144 mm. The projectile penetrated at a speed about equal to the impact velocity in the initial penetration and decelerated rapidly over since. This initial phenomenon was in agreement with the result obtained by high-speed photography as was stated previously in section 3.1.
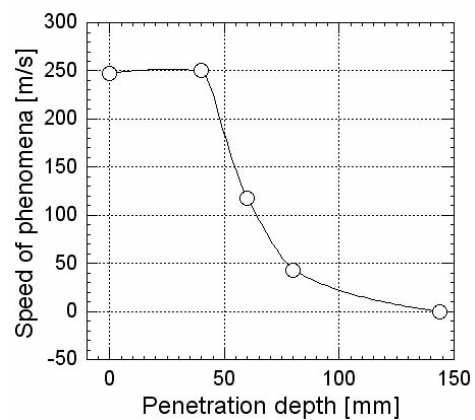

Fig.19 Example of result obtained by
optical glass fiber detector.
Impact velocity; 250 m/s,
penetration depth; 144 mm.

4. SUMMARY AND CONCLUSION

In order to establish tangible experimental methods and data analyzing methods to grasp various phenomena induced by high-speed impact of projectile on sand, the plate impact experiments were conducted using vertical powder gun. The major results are summarized as follows:

1. Sands around the penetrated projectile were smashed to fine powder of 5 μm or less like a potato starch.
2. Circumferential crashed sands were conically distributed and generated at impact velocity above 300 m/s.
3. Conical massive crashed sand was produced ahead of projectile and vertical angle converged to around 60° as the velocity increases.
4. The projectile penetrated at a speed about equal to the impact velocity in the initial penetration and decelerated rapidly over since.

References

1. Allen, W.A., Mayfield, E.B., Morrison, H.L., Dynamics of a Projectile Penetrating Sand, *Journal of Applied Physics*, 1957, 28(3), 370-376.
2. Allen, W.A., Mayfield, E.B., Morrison, H.L., Dynamics of a Projectile Penetrating Sand. Part II, *Journal of Applied Physics*, 1957, 28(11), 1331-1335.
3. Lyubin, L.Y., Povitzkii, A.S., Oblique Impact of a Solid on Soils, *Journal of Applied Mechanics and Technical Physics*, 1966, 1, 55-60.
4. Savvateev, A.F., Budin, A.V., Kolikov, V.A., Rutberg, PH.G., High-Speed Penetration into Sand, *International Journal of Impact Engineering*, 2001, 26, 675-681.
5. Chen, X.W., Li, Q.M., Deep Penetration of a Non-Deformable Projectile with Different Geometrical Characteristics, *International Journal of Impact Engineering*, 2002, 27, 619-637.
6. Bragov, A.M, Lomunov, A.K., Sergeichev, I.V., Tsembelis, K, Proud, W.G., Determination of Physicomechanical Properties of Soft Soils from Medim to High Strain Rates, *International Journal of Impact Engineering*, 2008, 35, 967-976.
7. Brog, J.P., Volger, T.J., Mesoscale Simulations of a Dart Penetrating Sand, *International Journal of Impact Engineering*, 2008, 35, 1435-1440.
8. Sultanov, V.G., Kim, V.V., Lomonosov, I.V., Shutov, A.V., Fortov, V.E., Numerical Modeling of Deep Impact Experiment, *International Journal of Impact Engineering*, 2008, 35, 1816-1820.